EFFECT OF LACTYL-DECORATED NANOCELLULOSE (NCLA) ON THE PROPERTIES OF PLA/PHBV/NCLA NANOCOMPOSITES

Cătălina-Diana UŞURELU[1], Gabriela-Mădălina OPRICĂ[2], Denis Mihaela PANAITESCU[3,*], Adriana Nicoleta FRONE[4], Cristian Andi NICOLAE[5], Augusta Raluca GABOR[6], Mircea TEODORESCU[7]

Biobased and biodegradable nanocomposites containing biopolymers as matrix and nanocellulose (NC) as a reinforcing agent are extensively studied as a sustainable alternative to traditional petroleum-based plastics for packaging, engineering and biomedical applications. However, a good dispersion of the hydrophilic NC in hydrophobic polymeric matrices remains a great challenge. Here, a lactyl-decorated nanocellulose (NCLA) was used as a modifier in a polylactic acid/poly(3-hydroxybutyrate-co-3-hydroxyvalerate) (PLA/PHBV) (50:50 weight ratio) matrix to improve its thermal and mechanical properties. Compared to the unmodified NC, NCLA showed better dispersion in the biopolymeric matrix and improved its properties. The addition of 1% NCLA to the PLA/PHBV matrix increased its storge modulus by 6 to 39%, depending on the temperature, with a 10% increase at room temperature. Similarly, the temperature at maximum degradation rate increased from 307.8 °C for the neat matrix to 318.4 °C for the nanocomposite containing 1% NCLA but decreased to 306.0 °C for the nanocomposite with 1% unmodified NC. The proposed PLA/PHBV/NCLA materials emerge as promising alternatives to traditional plastics.

Keywords: cellulose nanofibers, polylactic acid, polyhydroxyalkanoate, hydrophobization, nanocomposite

[1] PhD student, National Institute for Research and Development in Chemistry and Petrochemistry – ICECHIM Bucharest and Faculty of Chemical Engineering and Biotechnology, National University of Science and Technology POLITEHNICA Bucharest, Romania, e-mail: catalina.usurelu@icechim.ro

[2] PhD student, National Institute for Research and Development in Chemistry and Petrochemistry – ICECHIM Bucharest and Faculty of Chemical Engineering and Biotechnology, National University of Science and Technology POLITEHNICA Bucharest, Romania, e-mail: madalina.oprica@icechim.ro

[3]* PhD Eng., National Institute for Research and Development in Chemistry and Petrochemistry – ICECHIM Bucharest, Romania, corresponding author: e-mail: panaitescu@icechim.ro

[4] PhD Eng., National Institute for Research and Development in Chemistry and Petrochemistry – ICECHIM Bucharest, Romania, e-mail: adriana.frone@icechim.ro

[5] Eng., National Institute for Research and Development in Chemistry and Petrochemistry – ICECHIM Bucharest, Romania, e-mail: cristian.nicolae@icechim.ro

[6] Eng., National Institute for Research and Development in Chemistry and Petrochemistry – ICECHIM Bucharest, Romania, e-mail: raluca.gabor@icechim.ro

[7] Prof., Department of Bioresources and Polymer Science, Faculty of Chemical Engineering and Biotechnology, National University of Science and Technology POLITEHNICA Bucharest, e-mail: mircea.teodorescu@upb.ro

1. Introduction

Biobased and biodegradable polymers are increasingly seen as a sustainable alternative to traditional petroleum-based polymers and a solution to the large accumulation of non-biodegradable plastic waste in the environment [1]. Among biobased polymers, polylactic acid (PLA) and poly(3-hydroxybutyrate) (PHB) have received the most attention due to their advantages related to biodegradability, biocompatibility and non-toxicity, mechanical properties similar to those of other commodity polymers, and good melt processability and colorability [2,3]. However, both polymers show poor flexibility and high brittleness along with inadequate thermal stability [4,5], deficiencies that make their application in many areas difficult.

Blending PLA with PHB or poly(3-hydroxybutyrate-co-3-hydroxyvalerate) (PHBV) was proposed as a facile route to improve the properties of both biopolymers and to obtain blends with faster biodegradation, higher recrystallization ability and flexibility, higher oxygen barrier properties, and water resistance [5,6]. It has been reported that PHB addition led to an increase in PLA's crystallinity, while PLA increased PHB's stiffness [7]. However, in general, the simple blending PLA with PHB or PHBV did not lead to the expected high-performance materials due to the poor interface and loss of mechanical strength [6]. Therefore, reinforcing PLA/PHB or PLA/PHBV blends with biobased nanoparticles or nanofibers has emerged as a popular technique to improve their thermal, mechanical, or barrier properties [8-10]. In most works, a weight ratio between 75:25 and 70:30 was used for the PLA/PHB or PLA/PHBV matrix of the composites, because it was considered that such a composition provides the best properties for the blend and, subsequently, for the composite containing NC [7-11]. In particular, the addition of surface functionalized cellulose nanocrystals (CNCs) by TEMPO-mediated oxidation in a PLA/PHBV matrix using a solution casting technique led to an increase in the flexural strength and oxygen barrier properties of the nanocomposites with low content of cellulose nanocrystals (0.25 – 0.75 wt%) [8]. Similarly, the addition of 1.5 wt% cellulose nanofibers in a PLA/PHB blend using a masterbatch and melt mixing technique led to an important increase in the storage modulus regardless of the temperature and a delayed crystallization of PLA as revealed by the *in situ* X-ray diffraction analysis over a large temperature range [9]. Previous works have also shown that the surface modification of cellulose nanocrystals or nanofibers could improve their dispersion in the biopolymer matrix and, subsequently, the properties of the obtained nanocomposites [12,13]. However, the dispersion of surface-modified NC and its localization in the biopolymer matrix was not extensively studied although it could offer important information on the compatibility between the phases of these multicomponent systems. Therefore, in this work, nanocomposites from PLA, PHBV, and two types

of nanocelluloses, an unmodified NC prepared by the mechanical defibrillation of microcrystalline cellulose and a lactyl-decorated nanocellulose (NCLA), were obtained by melt blending. Based on previous works [2,3,8], the NCLA concentration in nanocomposites was varied from 0.5 to 2 wt%, knowing that lower nanocellulose concentrations lead to insignificant changes in properties, while higher concentrations of nanocellulose increase costs and lead to modest improvements or even a decrease in properties. To reduce the influence of the PLA/PHBV weight ratio on the dispersion and localization of nanocelluloses, a 50:50 ratio was used in this work for the PLA:PHBV polymer matrix. The influence of NC and NCLA on the morphology, thermal, and mechanical properties of the obtained bionanocomposites was studied by scanning electron microscopy (SEM), atomic force microscopy (AFM), thermogravimetric analysis (TGA), differential scanning calorimetry (DSC), and dynamic mechanical analysis (DMA). In this work, for the first time, a hydrophobized nanocellulose was studied as a modifier in an equi-component blend of the biobased polymers, PLA and PHBV. The new biomaterials obtained from PLA/PHBV reinforced with NCLA are promising alternatives to petroleum-based plastics for packaging, electronics, automotives, water purification, textiles, and biomedical applications.

2. Materials, methods, and experimental procedures

2.1. Materials

PLA granules with an L-lactide content of 98.6% were purchased from Nature Works LLC (USA) as PLA 4032D, PHBV powder (2% hydroxyvalerate) was acquired from Goodfellow (UK), and microcrystalline cellulose (MCC) from cotton linters was purchased from Sigma-Aldrich (USA). NC was obtained by passing aqueous MCC suspensions through a microfluidizer for 15 cycles, followed by freeze drying, while NCLA was obtained according to the methodology of Usurelu et al. [14], using a concentration of HCl catalyst of 0.05 M. The degree of substitution (DS) of the employed NCLA determined by the method described in [14] was ~0.15.

2.2. Preparation of the nanocomposites

The BP nanocomposites were obtained by the melt mixing of equal amounts of PLA and PHBV for 1 min in a Brabender mixing chamber at 165 °C and 50 rpm, followed by the addition of NC or NCLA and continuing the mixing for a total mixing time of 8 min. The PLA/PHBV/NCLA nanocomposites with 0.5, 1, and 2 wt% NCLA were denoted as BP_0.5NCLA, BP_1NCLA, and BP_2NCLA, while the PLA/PHBV/NC nanocomposite with unmodified NC was denoted as BP_1NC. A PLA/PHBV (50:50) blend was obtained in the same conditions and denoted as BP. The films used for characterization were obtained by compression molding in

a Dr. Collin press P200E (Germany) at 165 °C and 10 MPa for 60 s, the samples having been previously preheated at the same temperature for 120 s.

2.3. Characterization

The thermal behavior of the BP nanocomposites was investigated by TGA from 40 °C to 750 °C, at 10 °C/min heating rate, under nitrogen atmosphere (40 mL/min), and using a TA Q5000 thermobalance (TA Instruments Inc., USA). The calorimetric analysis was carried out on a DSC Q2000 analyzer (TA instruments, USA) by heating the sample from −70 °C to 220 °C, cooling it to −70 °C, and heating it again to 220 °C, at a heating/cooling rate of 10 °C/min. After each cycle, the temperature was equilibrated for 3 min.

The dynamic mechanical properties of the composites were evaluated using a DMA Q800 (TA Instruments, USA), multi-frequency - strain module, from −40 °C to 105 °C, at a frequency of 1 Hz and a heating rate of 3 °C/min, on specimens with the length × width × thickness of 12.8 mm × 6.5 mm × 0.25 mm.

A tabletop scanning electron microscope Hitachi TM4000 Plus II (Japan) was utilized for the morphological characterization of the cryo-fractured nanocomposite cross-sections, at an accelerating voltage of 10 kV, using the backscattered-electron detector. Prior to the measurements, the samples were coated with a nanometric layer of gold. Complementary morphological analysis on the surface of the samples was carried out by AFM in Peakforce Quantitative Nanomechanical Mapping mode using a MultiMode 8 microscope from Bruker (USA) and silicon tips with a resonance frequency of 40 kHz.

3. Results and discussion

3.1. DSC analysis

Fig. 1 reveals the thermal behavior of the PLA and PHBV controls, PLA/PHBV blend and nanocomposites, when heating-cooling-heating cycles were applied to the samples. The most important parameters were collected in Table 1. A very weak glass transition event at −2 - 0 °C, which is attributed to the amorphous PHBV component (T_{gPHBV}) [15], followed by a more visible glass transition at 58 °C, which is characteristic to the amorphous PLA [16,17], were observed in all the samples during the first heating cycle. A cold crystallization event at about 90 °C (T_{cc1}), present in all samples with different intensities, partially overlapped the glass transition of PLA (Fig. 1A). This event can be attributed to the PLA component, which is almost amorphous after processing, and crystallizes during heating [17]. Multiple melting peaks ($T_{m1(I,II,III)}$) were observed for all samples during the first heating cycle (Fig. 1A), with the second or third peak appearing in some cases only as shoulders. There are no significant differences in the melting temperatures between the blend and the nanocomposites, regardless of the nanocellulose content, however, attributing them is difficult. The DSC curves of the control samples, PLA

and PHBV, during the first heating cycle (Fig. 1D), show two endothermic peaks for PLA, similar as position with the first and second peaks of the nanocomposites, and two peaks for PHBV one close to the second peak of nanocomposites and the other at a lower temperature, while the third peak observed at the highest temperature in the DSC thermograms of the nanocomposites seems to have no correspondent. It is obvious that both PLA and PHBV have mutually influenced their melting and crystallization behaviors, which led to the appearance of larger crystal fractions with higher melting temperatures. This is most obvious in the case of PHBV. A similar behavior was reported by Zhang and Thomas for a PLA/PHB (50:50) blend [11]. They attributed the highest temperature peak to the melting of the PHB re-crystallized during heating [11].

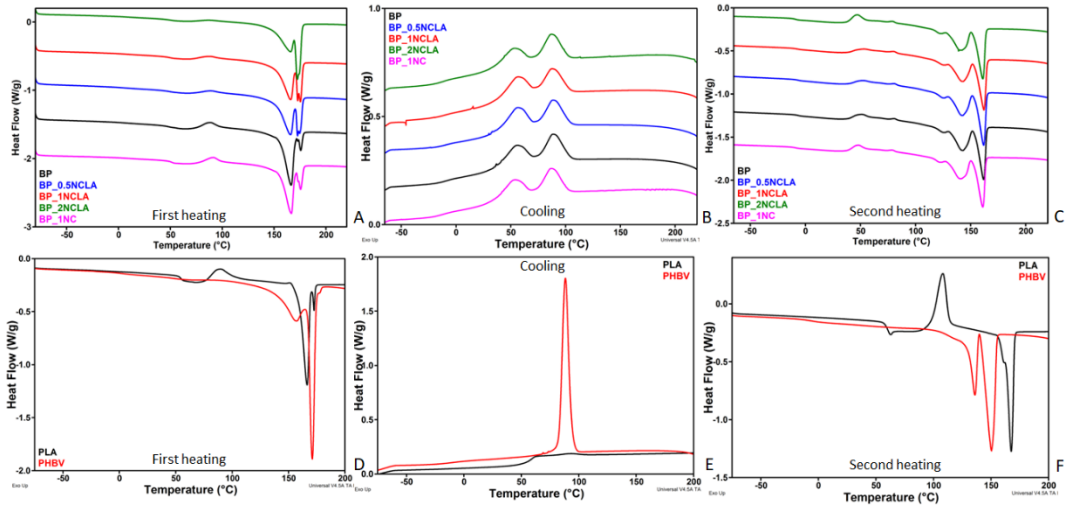

Fig. 1. DSC - first heating (A, D), cooling (B, E), and second heating (C, F) cycles for the nanocomposites (BP, BP_0.5NCLA, BP_1NCLA, BP_2NCLA, BP_1NC) and the PLA and PHBV controls

Comparing the area under the second and third peaks with that under the first one (A_{II+III}/A_I) for all samples, it may be observed this ratio increases with increasing the NCLA's concentration in nanocomposites. Therefore, NCLA potentiated this effect of larger crystal formation due to its nucleating activity, which was previously reported for some PLA/NC or PHBV/NC nanocomposites [3]. This effect was not observed in the case of BP-1NC, therefore, in contrast to NCLA, unmodified NC did not show a significant nucleating effect. In addition, the higher values of the melting enthalpy for the nanocomposites with NCLA as compared to those for BP and BP_1NC, support the idea that NCLA acted as an efficient nucleating agent in the PLA/PHBV/NCLA nanocomposites.

Table 1

Parameters determined from the DSC curves for the BP, the BP_0.5NCLA, BP_1NCLA, BP_2NCLA, BP_1NC samples, and PLA and PHBV controls

Sample	T_{gPHBV} (°C)	T_{cc1} (°C)	$T_{m1(I,II,III)}$ (°C)	ΔH_{m1} (J/g)	T_c (°C)	T_{cc2} (°C)	$T_{m2(I,II)}$ (°C)	ΔH_{m2} (J/g)
BP	-1.4	88.7	166.4/172.8/175.7	58.4	55.4/88.3	50.6/81.0	142.5/161.7	54.3
BP_0.5NCLA	-1.0	89.6	165.8/172.6/174.6	62.2	56.1/88.1	51.7/81.0	140.9/160.9	54.1
BP_1NCLA	-0.6	88.5	165.7/172.7/175.4	61.6	53.7/86.7	52.5/80.4	142.2/161.7	53.7
BP_2NCLA	-1.7	88.8	165.8/172.4/174.1	63.4	56.0/87.3	46.8/79.3	142.0/162.0	54.0
BP_1NC	-1.4	91.6	166.5/173.1/175.6	56.9	53.4/86.5	47.9/79.1	140.7/161.0	51.4
PLA	-	89.1	166.4/172.5	42.2	-	108.2	167.6	39.4
PHBV	-0.5	-	157.0/171.1	92.8	88.3	-	136.0/150.4	78.4

The DSC curves recorded during the cooling step (Fig. 1B) show two distinct peaks comparable in terms of peak area, the first at about 55 °C and the second at 87-88 °C. However, only neat PHBV crystallizes during cooling with a sharp crystallization peak (T_c) at 88 °C (Fig. 1E), while the assignment of the exothermic peak at 55 °C is difficult. It cannot be attributed to PLA crystallization because at this temperature PLA exhibits a glass transition event. One possibility is the T_{cPHBV} shift to a lower temperature, probably influenced by PLA or some degradation phenomena, and the attribution of the higher temperature peak to PLA. It may be presumed that PHBV, which was added as powder to PLA, determined a significant increase in shear and in the temperature of the melt during processing, leading to a reduction in the number of nucleation sites [18] and degradation phenomena. Indeed, Bossu et al. [18], which studied the effect of the processing temperature on the PHBV crystallization, reported a strong decrease in the T_c, from 106 to 73 °C, when the pre-heating temperature increased from 150 to 180 °C. They explained this behavior by the elimination of residual nuclei, which caused the crystallization process to begin at a lower temperature.

All samples have similar melting behavior during the second heating cycle (Fig. 1C). Unlike the first heating, two new small exothermic events appear in the second heating at about 50 and 80 °C, which can be caused by the cold crystallization of PHBV [19] and PLA [3], respectively. The DSC thermograms of the control samples recorded during the second heating cycle (Fig. 1F) highlight the cold crystallization of PLA which appears as clearly defined exothermic peak. One aspect that should be remarked is the decrease in the $T_{m2(I,II)}$ by more than 10 °C as compared to the first heating cycle ($T_{m1(I,II,III)}$). A similar decrease in the T_m was noted for the PHBV control, while for PLA the decrease was not as important (Table 1). These data suggest the fact that some degradation processes occurred not only during the melt processing step but also during the first heating and subsequent cooling of the samples, which could lead to a decrease in the molecular weight of the biopolymers [20].

3.2. Thermogravimetric analysis

The thermogravimetric and differential thermogravimetric curves of the PLA and PHBV controls and the BP samples are shown in Fig. 2A,B, while the thermal parameters determined from the TG-DTG curves are depicted in Table 2.

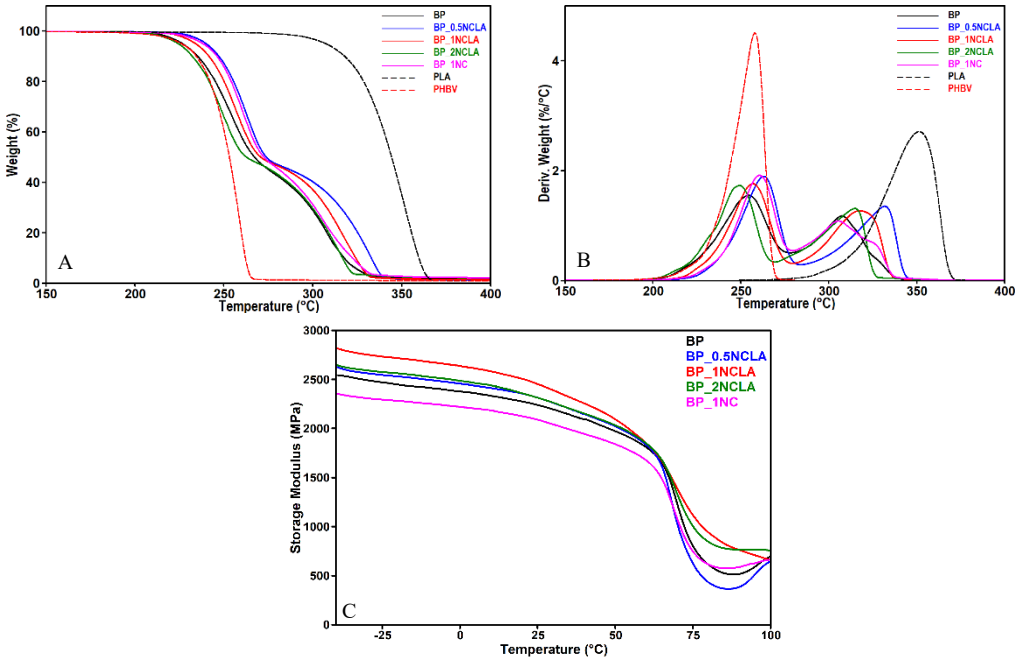

Fig. 2. TG and DTG curves for the PLA and PHBV controls, BP blend and nanocomposites (A and B); Storage modulus vs. temperature curves of the BP samples (C);

Table 2

The thermal characteristics of the BP samples determined from the TG and DTG curves

Sample	T_{on} (°C)	$T_{5\%}$ (°C)	T_{max1} (°C)	T_{max2} (°C)	$R_{700°C}$ (%)
BP	232.9	226.7	253.7	307.8	0.3
BP_0.5NCLA	245.3	239.9	262.8	332.0	0.3
BP_1NCLA	239.4	234.1	256.5	318.4	0.3
BP_2NCLA	230.8	224.4	249.0	315.0	0.7
BP_1NC	244.2	238.3	260.2	306.0	0.7
PLA	326.1	307.4	-	351.3	0.1
PHBV	241.7	226.2	257.9	-	0.5

The PLA and PHBV controls exhibit single-stage degradation with the temperature of the maximum degradation rate (T_{max}) at 351 and 258 °C, respectively. Unlike the control samples, the blend and nanocomposites exhibit two-stage degradation, with a T_{max1}, which corresponds to the PHBV phase, slightly lower or close to that of neat PHBV, and a T_{max2}, which corresponds to the PLA

phase, much lower than that of the PLA control. As it can be observed, blending PLA with PHBV at this ratio led to a decrease in the decomposition temperatures, especially for the PLA component, which explains some of the DSC results. Similar observations were reported for a PLA/PHBV 55:45 blend [21]. The addition of 0.5 or 1 wt% NCLA in the blend increased its onset degradation temperature (T_{on}), the temperature at 5% weight loss ($T_{5\%}$), and the T_{max} values, but, in general, a higher concentration of NCLA decreased them (Table 2), similar to other observations [22, 23]. The residue at 700 °C ($R_{700°C}$) was lower than 1% for all the samples.

3.3. DMA results

The viscoelastic properties of the BP samples were studied by DMA, and the variation of the storage modulus (E') with temperature is shown in Fig. 2C. The blend and nanocomposites show small variations in the E' value at temperatures below the glass transition (T_g) of PLA (70 °C), because the influence of the amorphous PHBV, whose T_g is around 25 °C [24], is small, being a consequence of the high crystallinity of PHBV [5]. A strong decrease in the E' value is observed at 68 - 70 °C, due to the glass transition of PLA, which is followed by a slight increase in the E', marking the beginning of cold crystallization of PLA [9].

The addition of NCLA led to an increase in E' (Table 3), which was higher than that of the blend, regardless of the temperature. This shows the reinforcing effect of the NCLA and the influence of the surface treatment of nanocellulose on the mechanical properties of the nanocomposite. In contrast, the addition of unmodified NC to the blend led to a decrease in E', regardless of temperature. The different effects of NC and NCLA show the great influence of the treatment in compatibilizing the blend and increasing its storage modulus.

Table 3

Storage modulus (E') and $T_{g\,(PLA)}$ determined from the DMA curves for the BP samples

Sample	$E'_{-25°C}$, MPa	$E'_{0°C}$, MPa	$E'_{25°C}$, MPa	$E'_{50°C}$, MPa	$E'_{75°C}$, MPa	T_{gPLA} (°C)
BP	2471	2378	2240	1974	804	69.9
BP_0.5NCLA	2546	2457	2314	2023	625	68.2
BP_1NCLA	2733	2639	2454	2094	1118	69.2
BP_2NCLA	2576	2487	2315	2033	1005	69.4
BP_1NC	2294	2221	2090	1840	748	68.8

3.4. Morphological analysis by SEM and AFM

Fig. 3 shows the SEM images of the PLA/PHBV (50:50) blend and nanocomposites' cross-sections at two different magnifications.

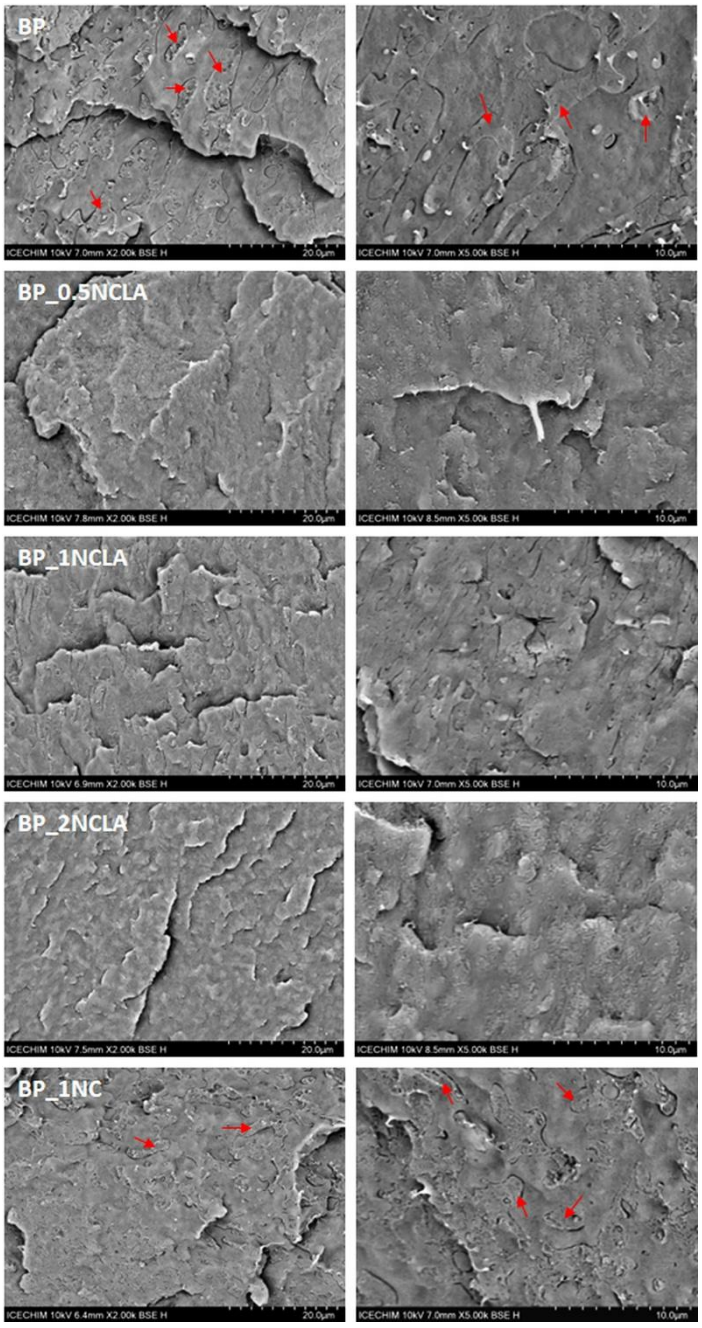

Fig. 3. SEM images of the BP, BP_0.5NCLA, BP_1NCLA, BP_2NCLA, and BP_1NC samples at ×2000 (left) and ×5000 (right) magnification; rougher islands were marked by red arrows

The BP blend shows a two-phase morphology, with rough elongated islands dispersed between smoother areas. The two-phase morphology, which is a

characteristic of immiscible blends, was expected at this PLA:PHBV ratio, knowing that the miscible morphology of this blend at an 85:15 ratio turns into an immiscible one at a lower PLA:PHBV ratio [25]. The assignment of the two phases is facilitated by the different crystallinity of PHBV (highly crystalline) and PLA (largely amorphous). Therefore, the rougher islands contain the highly crystalline PHBV, while the smother areas contain the amorphous PLA. The morphology is close to a continuous one, which is expected for a 50:50 weight ratio of the components in immiscible blends [26], however, the slight difference between the melt density of the two phases, 1.25 g/cm^3 for PHBV [27] and ~1.1 g/cm^3 for PLA [28] favors the appearance of rough PHBV islands dispersed in a more continuous PLA phase. The morphology of the nanocomposites is different, with the separation between the rough islands and the smooth areas strongly diminishing and becoming even more difficult to be detected as the concentration of NCLA in the nanocomposites increases. However, the SEM images of BP_1NC are similar to those of the blend and not to those of the BP_NCLA nanocomposites, the morphology with elongated islands being maintained in this case. This behavior suggests a double effect of NCLA in the nanocomposites, as a reinforcing agent, according to the DMA results, and as a compatibilizer, according to the SEM images, that leads to increased miscibility between PLA and PHB and a better dispersion of the two components in nanocomposites. Due to their nanometer size and the lack of large agglomerations, the NC and NCLA nanofibers cannot be detected in the SEM images at these magnifications, which are however, required for observing the large size of the PLA and PHBV phases, ranging from a couple of microns to about 10 μm (Fig. 3).

Higher magnification SEM images of BP_1NC and BP_2NCLA, the nanocomposite with the best dispersion of the components, are displayed in Fig. 4A and B. Rougher islands and NC agglomerated fibers, clearly detached from the matrix (marked by red circles), are frequently observed in the SEM image of BP_1NC (Fig. 4A), but well dispersed nanofibers and no distinction between PLA and PHBV phases is seen in the SEM image of BP_2NCLA (Fig. 4B). The large holes between the agglomerations of NC fibers and the matrix indicate poor adhesion at the interface [23]. Such holes were not observed in the case of the NCLA-reinforced nanocomposites. This different behavior shows the remarkable effect of the "lactyl" modification of NC, which, on the one hand, increases the hydrophobicity of NC improving its dispersion in the biopolimeric matrix, and, on the other hand, enhances the miscibility of PLA and PHBV in the nanocomposites. Notably, even at a relatively low DS of ~0.15, the chemical modification with lactyl groups resulted in a significantly improved dispersion of the NC nanofibers within the PLA/PHBV matrix. Although higher DSs could have further enhanced the dispersion of the cellulose nanofibers within the polymer matrix, such DSs are typically achieved under harsher reaction conditions and using solvents for NC

more potent than water, which would have taken from the environmental friendliness, simplicity and accessibility of the chemical modification procedure we proposed in [14]. In addition, the use of harsher reaction conditions and stronger solvents for cellulose, as well as higher DSs usually alter the crystallinity [29], thermal and mechanical properties of nanocellulose [30], which could affect its reinforcing capabilities. Similarly to our study, Wang et al. [31] showed that low DSs of 0.035 and 0.20 obtained by the esterification of CNCs with L-malic acid were sufficient to produce important improvements in the mechanical resistance and thermal stability of poly(methyl methacrylate) (PMMA), as well as to enhance the dispersibility of CNCs within the PMMA matrix, when the modified CNCs content in the nanocomposites was 1 wt%.

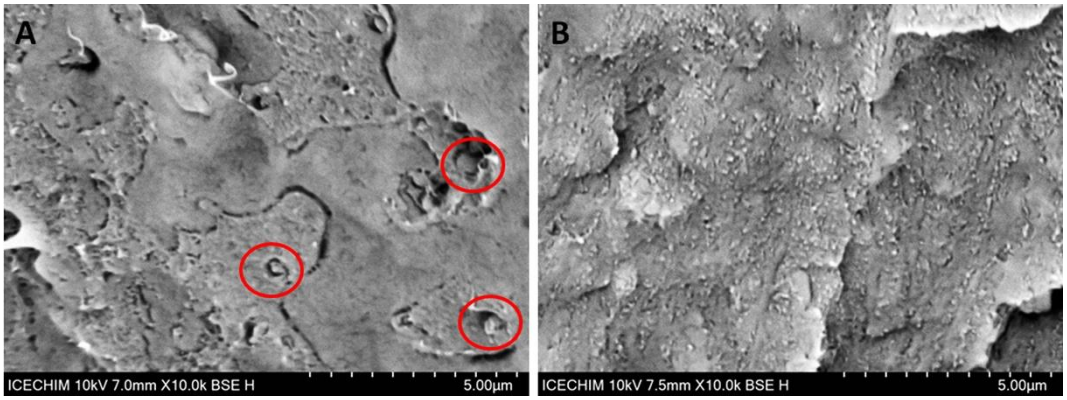

Fig. 4. SEM images (×10000) of the BP_1NC (A) and BP_2NCLA (B); agglomerated NC fibers were marked by red circles

For a better insight on the size of NCLA and NC in the nanocomposites and their dispersion, AFM analysis was carried out on the surface of BP_1NCLA and BP_1NC films (Fig. 5). In the topographic images of the nanocomposites, NCLA and NC appear as light-colored areas or mounds. Comparing the diameter of these light objects, 20 – 80 nm in the case of BP_1NCLA, and between 50 nm and several hundreds of nm in the case of BP_1NC, it is obvious that NCLA are smaller in diameter and better dispersed than NC, which shows frequently agglomerations. These observations are in line with the remarks on the higher magnification SEM images (Fig. 3) and previously reported AFM results on PLA films containing PLA-grafted lignin nanoparticles compared to PLA with unmodified lignin nanoparticles [32].

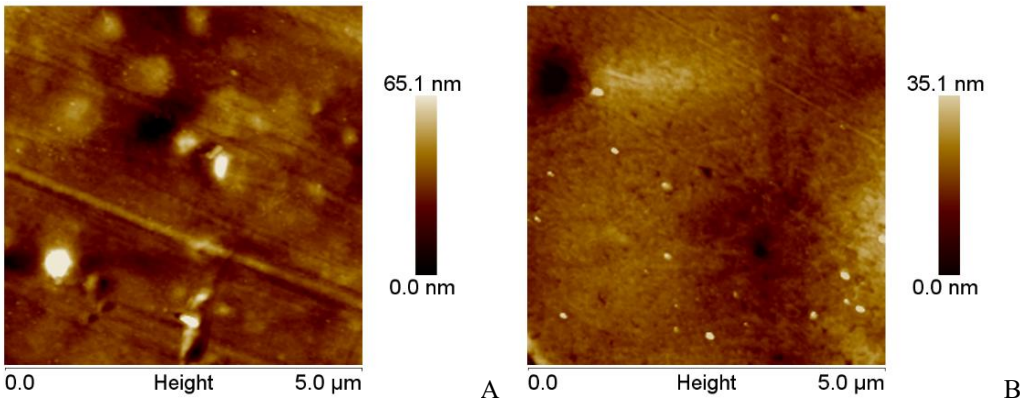

Fig. 5. AFM - topographic images of the BP_1NC (A) and BP_1NCLA (B) samples

It should be remarked that NCLA has diameters lower than 100 nm and a good dispersion in the biopolymeric matrix, which makes the new BP_NCLA materials fit perfectly into the category of nanocomposites.

4. Conclusions

All bio-based nanocomposites were successfully prepared by the addition of unmodified or lactyl-decorated nanocellulose into a 50:50 PLA:PHBV blend. When used in small concentrations (0.5 and 1 wt%), NCLA accelerated the crystallization and improved the thermal stability and mechanical strength of the blend, while the SEM images revealed that NCLA is an effective compatibilizing agent, that increases the miscibility between PLA and PHBV. In contrast, NC exhibited a less pregnant nucleating action and improving effect on the thermal stability of the blend and led to a reduction in its mechanical strength. Additionally, the SEM showed that NC displayed no visible compatibilizing effect on the PLA and PHBV phases. Considering the beneficial effects of NCLA on the properties of the 50:50 PLA:PHBV blend, NCLA emerges as a promising additive capable of functioning both as a reinforcing agent and as a compatibilizer between the otherwise immiscible PLA and PHBV biopolymers.

Acknowledgment:

This study was funded by the Ministry of Research, Innovation and Digitization, CNCS—UEFISCDI, through the project PN23.06.01.01/2022 AquaMat, within PN23.06 Core Program.

REFERENCES

[1] *A. George et al.*, A comprehensive review on chemical properties and applications of biopolymers and their composites, Int. J. Biol. Macromol., Vol. **154**, pp. 329-338, 2020, DOI: 10.1016/j.ijbiomac.2020.03.120.

[2] *C.D. Usurelu et al.*, Poly(3-hydroxybutyrate) nanocomposites with cellulose nanocrystals, Polymers, Vol. **14,** Iss. 10, 1974, 2022, DOI: 10.3390/polym14101974.
[3] *H. Chai et al.*, The fabrication of polylactide/cellulose nanocomposites with enhanced crystallization and mechanical properties, Int. J. Biol. Macromol., Vol. **155**, Iss. 8, pp. 1578-1588, 2020, DOI: 10.1016/j.ijbiomac.2019.11.135.
[4] *D. Huo et al*., Modified nano-lignocellulose preparation by azolidinone and its application in polylactic acid composite film and paper coating, Ind. Crops Prod., Vol. **223**, 120151, 2025, DOI: 10.1016/j.indcrop.2024.120151
[5] *M.S. Popa et al*., Polyhydroxybutyrate blends: a solution for biodegradable packaging?, Int. J. Biol. Macromol., Vol. **207**, Iss. 10, pp. 263-277, 2022, DOI: 10.1016/j.ijbiomac.2022.02.185.
[6] *X. Li et al*., Efficient fabrication of PLA/PHB composites with enhanced mechanical properties, excellent thermal stability, fast crystallization ability, and degradation rate via the synergistic of weak shear field and melt quenching technique, Ind. Crops Prod., Vol. **196**, 116516, 2023, DOI: 10.1016/j.indcrop.2023.116516.
[7] *M.P. Arrieta et al*., Multifunctional PLA–PHB/cellulose nanocrystal films: Processing, structural and thermal properties, Carbohydr. Polym., Vol. **107**, pp.16-24, 2014, DOI: 10.1016/j.carbpol.2014.02.044.
[8] *Y.K. Dasan et al*., Polymer blend of PLA/PHBV based bionanocomposites reinforced with nanocrystalline cellulose for potential application as packaging material, Carbohydr. Polym., Vol. **157**, pp. 1323-1332, 2017, DOI: 10.1016/j.carbpol.2016.11.012.
[9] *A.N. Frone et al*., Poly(lactic acid)/poly(3-hydroxybutyrate) biocomposites with differently treated cellulose fibers, Molecules, Vol. **27**, Iss. 8, 2390, 2022, DOI: 10.3390/molecules27082390.
[10] *A.N. Frone et al.*, Morpho-Structural, Thermal and Mechanical Properties of PLA/PHB/Cellulose Biodegradable nanocomposites obtained by compression molding, extrusion, and 3D printing, Nanomaterials, Vol. **10**, Iss. 1, 51, 2020, DOI: 10.3390/nano10010051.
[11] *M. Zhang et al.*, Blending polylactic acid with polyhydroxybutyrate: The effect on thermal, mechanical, and biodegradation properties, Adv. Polym. Technol., Vol. **30,** Iss. 2, pp. 67-79, 2011, DOI: 10.1002/adv.20235.
[12] *K. Li et al.*, Surface-modified and oven-dried microfibrillated cellulose reinforced biocomposites: Cellulose network enabled high performance, Carbohydr. Polym., Vol. **256,** 117525, 2021, DOI: 10.1016/j.carbpol.2020.117525.
[13] *A. Chakraborty, P. Ghalsasi, P. Radha.*, Green Engineering: Poly (lactic acid) Composite Materials Fortified with Surface-Modified Nanocellulose from *Borassus flabellifer* Leaves. *Biomass Conv. Bioref.* Vol. **15**, pp. 6871–6888, 2025, DOI: 10.1007/s13399-024-05670-7.
[14] *C.D. Usurelu et al.*, Preparation and functionalization of cellulose nanofibers using a naturally occurring acid and their application in stabilizing linseed oil/water Pickering emulsions, Int. J. Biol. Macromol., Vol. **262**, Iss. 7, 129884, 2024, DOI: 10.1016/j.ijbiomac.2024.129884.
[15] *D.M. Panaitescu et al*., Biocomposite foams based on polyhydroxyalkanoate and nanocellulose: morphological and thermo-mechanical characterization, Int. J. Biol. Macromol., Vol. **164,** pp. 1867-1878, 2020, DOI: 10.1016/j.ijbiomac.2020.07.273.
[16] *S.K. Bhattacharjee et al*., Impact of nano-silica on thermal, mechanical, and rheological properties of melt-extruded PLA-based nanocomposites, Int. J. Biol. Macromol., Vol. **321**, 146077, 2025, DOI: 10.1016/j.ijbiomac.2025.146077.
[17] *A.N. Frone et. al*., Thermal and mechanical behavior of biodegradable polyester films containing cellulose nanofibers, J. Therm. Anal. Calorim., Vol. **138**, Iss. 4, pp. 2387–2398, 2019, DOI: 10.1007/s10973-019-08218-4

[18] *J. Bossu et al*., Impact of the processing temperature on the crystallization behavior and mechanical properties of poly[R-3-hydroxybutyrate-co-(R-3-hydroxyvalerate)], Polymer, Vol. **229,** 123987, 2021, DOI: 10.1016/j.polymer.2021.123987.

[19] *R.M.R. Wellen, E.L. Canedo, M.S. Rabello*, Melting and crystallization of poly (3-hydroxybutyrate)/carbon black compounds. Effect of heating and cooling cycles on phase transition, J. Mater. Res., Vol. **30**, pp. 3211–3226, 2015, DOI: 10.1557/jmr.2015.287.

[20] *H. Lu, H. Sato, S.G. Kazarian*, Effect of Tm of blend components on the isothermal melt-crystallization process of PHB/PLLA blends investigated using spectroscopic imaging and DSC, Polymer, Vol. **248**, 124820, 2022, DOI: 10.1016/j.polymer.2022.124820.

[21] *H. Zhao et al.*, Morphology and properties of injection molded solid and microcellular polylactic acid/polyhydroxybutyrate-valerate (PLA/PHBV) blends, Ind. Eng. Chem. Res., Vol. **52**, Iss. 7, pp. 2569-2581, 2013, DOI: 10.1021/ie301573y.

[22] *F. Luzi et al.*, Combined effect of cellulose nanocrystals, carvacrol and oligomeric lactic acid in PLA_PHB polymeric films, Carbohydr. Polym., Vol. **223**, 115131, 2019, DOI: 10.1016/j.carbpol.2019.115131.

[23] *P. Bazan et al.*, Composites based on PLA/PHBV blends with nanocrystalline cellulose NCC: mechanical and thermal investigation, Materials, Vol. **17**, 6036, 2024, DOI: 10.3390/ma17246036.

[24] *D. Nath et al.*, Green composites from plasticized poly(3-hydroxybutyrate-co-3-hydroxyvalerate) bioplastic and cellulosic fiber: Effect of compatibilizer and grafting percentage on interfacial adhesion and biocomposite performance, Int. J. Biol. Macromol., Vol. **315**, Iss. 21, 144107, 2025, DOI: 10.1016/j.ijbiomac.2025.144107.

[25] *H. Zhao et al.*, Processing and characterization of solid and microcellular poly(lactic acid)/polyhydroxybutyrate-valerate (PLA/PHBV) blends and PLA/PHBV/Clay nanocomposites, Compos. B Eng., Vol. **51**, pp. 79-91, 2013, DOI: 10.1016/j.compositesb.2013.02.034.

[26] *E.G.R. dos Anjos et al*., Tuning the morphology of immiscible polymer blend-based hybrid nanocomposite for improving microwave absorption response. ACS Polym. Au, Vol. **5**, Iss. 1, pp. 10-25, 2024, DOI: 10.1021/acspolymersau.4c00087.

[27] *V. Gigante et al.*, Utilization of coffee silverskin in the production of Poly(3-hydroxybutyrate-co-3-hydroxyvalerate) biopolymer-based thermoplastic biocomposites for food contact applications, Compos. - A: Appl. Sci. Manuf., Vol. **140**, 106172, 2021, DOI: 10.1016/j.compositesa.2020.106172.

[28] *Q. Ji et al.*, Study on the static and dynamic mechanical properties and constitutive models of 3D printed PLA and PLA-Cu materials, Mater. Today Commun., Vol. **39**, Iss. 1, 108690, 2024, DOI: 10.1016/j.mtcomm.2024.108690.

[29]. *A. Sato et al.*, Surface modification of cellulose nanofibers with alkenyl succinic anhydride for high-density polyethylene reinforcement, Compos. - A: Appl. Sci. Manuf., Vol. **83**, pp. 72-79, 2016, DOI: 10.1016/j.compositesa.2015.11.009.

[30]. *T.C. Mokhena, M.J. John*, Esterified cellulose nanofibres from saw dust using vegetable oil, Int. J. Biol. Macromol., Vol. **148**, pp. 1109-1117, 2020, DOI: 10.1016/j.ijbiomac.2020.01.278.

[31]. *W. Wang et al.*, Green functionalization of cellulose nanocrystals for application in reinforced poly(methyl methacrylate) nanocomposites, Carbohydr. Polym., Vol. **202**, pp. 591-599, 2018, DOI: 10.1016/j.carbpol.2018.09.019.

[32] *A. Boarino et al.*, Uniformly dispersed poly(lactic acid)-grafted lignin nanoparticles enhance antioxidant activity and UV-barrier properties of poly(lactic acid) packaging films, ACS Appl. Polym. Mater., Vol. **4**, pp. 4808-4817, 2022, DOI: 10.1021/acsapm.2c00420.